2008

Nanoscale Characterisation of Advanced High Strength Steels Using Atom Probe Tomography

E V. Pereloma
University of Wollongong, elenap@uow.edu.au

I. B. Timokhina
Deakin University

P. D. Hodgson
Deakin University

M. K. Miller
Oak Ridge National Laboratory, US

Nanoscale Characterisation of Advanced High Strength Steels Using Atom Probe Tomography

Elena V Pereloma[1], Ilana B Timokhina[2], Peter D Hodgson[2] and Michael K Miller[3]

[1]School of Mechanical, Materials and Mechatronics Engineering, University of Wollongong, Wollongong, Australia, NSW2500
[2]Centre for Material and Fibre Innovation, Deakin University, Geelong, Vic 3217, Australia
[3]Materials Science and Technology Division, Oak Ridge National Laboratory, TN 37831-6136, USA
E-mail: [1]elenap@uow.edu.au

Abstract

Over the last few years, there has been significant interest in the design of new high strength steels with complex microstructures and the manipulation of their properties at the nanoscale. Understanding the effects of alloying additions on the nanoscale level is essential for tailoring the steel composition and properties for a specific product requirement. Atom probe tomography plays an important role in the characterisation of the microstructural features at the atomic level. This powerful technique has been used for the direct experimental observations of early stages of phase transformations, clustering, fine precipitation, atmospheres around dislocations and segregation to boundaries. An overview on recent advances in the application of atom probe tomography to study thermomechanically processed transformation-induced plasticity steels and nanocrystalline bainitic steels is presented. Keywords: *Atom Probe Tomography, Advanced High Strength Steel, Thermomechanical Processing, Bake Hardening, Cottrell Atmosphere, Precipitation, Phase Transformation.*

INTRODUCTION

The continuous quest for higher strength steels forces engineers and scientists to seek new approaches towards design of new steel compositions and processing routes. Development of new advanced experimental techniques opened previously impossible avenues for design of compositions and microstructures at atomic scale. Recent advances in atom probe tomography, e.g. development of state-of-the-art voltage-pulsed and laser-pulsed local electrode atom probes [1–3], support this quest by providing the necessary information on atom interactions, solute segregation to dislocations, boundaries and other defects, redistribution of alloying elements between phases, cluster and precipitation formation. Based on the obtained information, a deeper understanding of the mechanisms of phase transformations and strengthening can be achieved, which is essential for progress in the development of advanced high strength steels. Fast data acquisition rates (2 million atoms in ~15 minutes) and substantial volumes analysed (~100 million atoms) allow the analysis of fine microstructural features with low density. This review paper is a comparison of our atom probe results obtained on transformation-induced plasticity (TRIP) steels [4–6] with those from Caballero *et al.* [7, 8] on nano-structured bainitic steel.

EXPERIMENTAL

Thermomechanically processed CMnSi Transformation-Induced Plasticity (TRIP) steels with and without additions of Nb, Mo and Al were examined using Transmission Electron Microscopy (TEM) and Atom Probe Tomography (APT). The compositions of the steels used are given in Table 1. Detailed descriptions of the Thermomechanical Processing (TMP) and experimental techniques are given elsewhere [4–6]. Details of processing and characterisation of high carbon, high silicon, nanostructured bainitic steel are described elsewhere [7, 8]. After processing, the TRIP steels were subjected to 4% pre-straining and bake hardening at 180^{o}C for 30 min., whereas the bainitic steel was tempered at 400–450^{o}C for 30 min. and 1 h.

Table 1: Steel compositions, at. %. Balance is Fe.

Steel	Non Nb	NbAl	NbMo	NbMoAl	Bainitic
C	0.95	0.996	0.96	0.95	4.34
Si	3.01	2.31	2.88	2.29	2.76
Mn	1.54	1.52	1.49	1.51	1.82
Nb	0.003	0.022	0.021	0.021	–
Mo	–	0.002	0.114	0.165	0.14
Al	0.02	1.15	0.02	1.15	–
Cu	0.003	0.026	0.017	0.026	–
P	–	0.048	0.044	0.048	–
Cr	–	–	–	–	1.28
V	–	–	–	–	0.09

An Imago Local Electrode Atom Probe (LEAP®) operated at a pulse repetition rate of 200kHz, 0.2 pulse fraction and with a sample temperature of 60K was used for atom probe analysis. All retained austenite in studied steels was deemed to be transformed to martensite at the examination temperature. Specimens were prepared by standard micro-electropolishing techniques [9]. The maximum separation envelope method [9] was used to estimate solute-enriched regions, such as segregations at dislocations, clusters and fine precipitates.

RESULTS AND DISCUSSION

Microstructure of Steels

As shown by Caballero et al. [7, 8], the microstructure of the bainitic steel after completion of isothermal bainite transformation at 200^{o}C comprises fine carbide-free bainite with nanolayers of retained austenite (Figure 1).

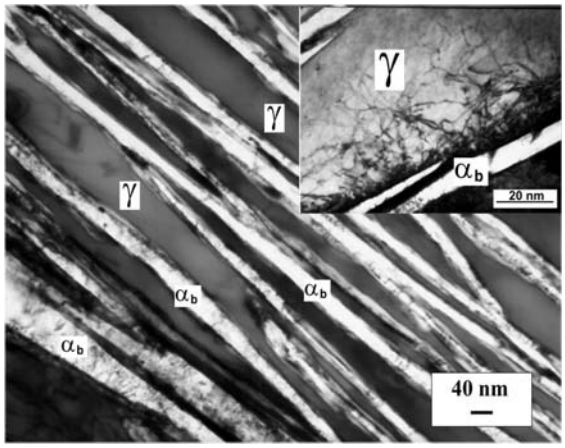

Figure 1: Thin foil TEM of bainitic steel. Reproduced from Caballero *et al.* [8], copyright 2008, with permission from Elsevier

The microstructure of TRIP steels after TMP consisted of ~50–55% polygonal ferrite (PF), ~30% of bainite (predominantly granular bainite (GB) or acicular ferrite (AF) depending on steel composition), 8–12% of retained austenite (RA) and remaining martensite (M) (Figure 2). In the alloyed TRIP steels, NbC and MoC precipitates were present (Figure 3).

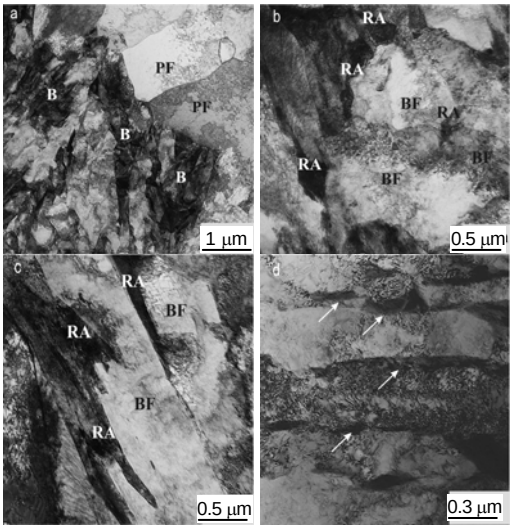

Figure 2: Representative TEM micrographs of the thermomechanically processed TRIP steels: general view (a), granular bainite (b), acicular ferrite (c) and upper bainite (d). PF—polygonal ferrite, BF- bainitic ferrite, B- bainite, RA—retained austenite. Arrows in d indicate iron carbides

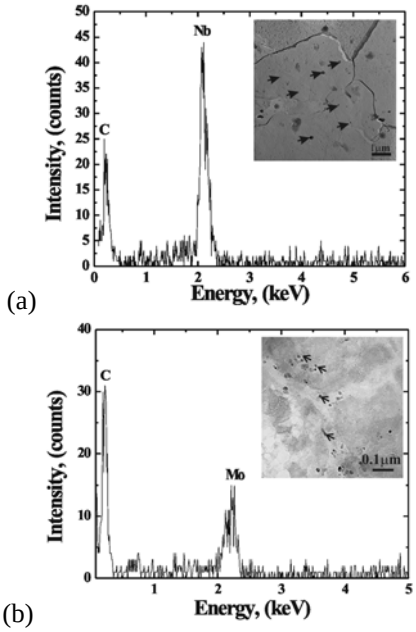

Figure 3: Representative energy dispersive X-ray spectra from NbC particles (a) and MoC particles (b) shown in carbon replica insets by arrows. Note: Ni peaks from the grid have been removed

Phase Composition Analysis

Examples of various phases observed by APT in TRIP steels and bainitic steel are shown in Figures 4–6. Compositional analysis of selected volumes allowed identification of phases based on generally accepted values of C content in these phases [6–8, 10, 11]: >0.07 at.% polygonal ferrite, 0.1–0.5 at.% bainitic ferrite (BF) and >2 at % retained austenite or martensite, both of which were martensite at the testing temperature.

The volume containing a lath of bainitic ferrite with cementite particles on each side, which could represent interlath carbides, is shown in Figure 4. Such a microstructure is assumed to be upper bainite. Although the concentration profile (Figure 4b) indicates only 14 at.% C within a carbide, a selected volume composition analysis positioned within the cylinder yielded a value of 21.7 ± 0.3 at.% C, which is close to the 25 at.% C content in Fe_3C.

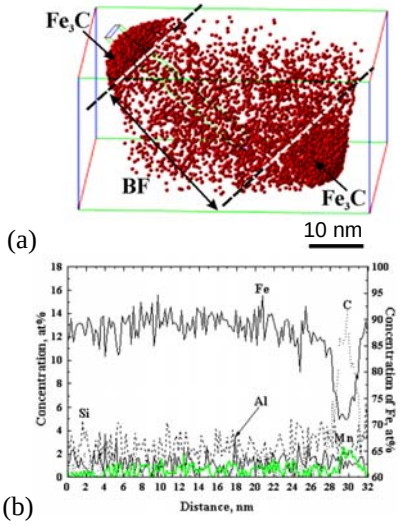

Figure 4: C atom map (a) and concentration profile across the bainitic ferrite/carbide interface (dashed lines) (b) showing upper bainite in the NbMoAl TRIP steel. BF- bainitic ferrite, Fe_3C indicates interlath carbides. Reprinted from [6], Copyright 2007, with permission from Elsevier

A selected volume containing two phases is shown in Figure 5: polygonal ferrite is on the left, and bainitic ferrite is on the right. From compositional analysis, the redistribution of various elements, for example Mn and Si, between phases is clear. The polygonal ferrite (PF) in Figure 5 has an average composition of 0.026 ± 0.002 C, 1.07 ± 0.06 Mn and 4.34 ± 0.02 Si (at.%), whereas C and Mn contents have increased to 0.25 ± 0.03 and 1.85 ± 0.01 at.%, respectively, in adjacent bainitic ferrite. At the same time, the Si level has decreased to 2.09 ± 0.1 at.%. Comparison of compositions of the parent (austenite) and product phases provides insight into the mechanism of phase transformation.

The most striking example is that in both the TRIP and bainitic steels, an excess of carbon in bainitic ferrite and similar content of substitutional elements in prior austenite and bainitic ferrite support the diffusionless mechanism [12–14] of bainite formation (Figures 5 and 6). The austenite/bainitic ferrite regions in the bainitic steel after various stages of processing are shown in Figure 6. The work of Caballero *et al.* [7] revealed that the C content in retained austenite and bainitic ferrite was in the range between 5 and 7 at.% and 0.5–0.62 at.%, respectively. Bainitic ferrite had much higher carbon level compared with that expected from para-equilibrium with austenite (~0.12 at.%) [7, 8, 15]. APT results by Caballero *et al.* [7] (Figures 6 (b)–(e)) also provide direct confirmation of the absence of any segregation at the austenite/BF interface and partitioning of substitutional elements between phases during bainite formation. This is in agreement with previous APT results [10, 11, 16].

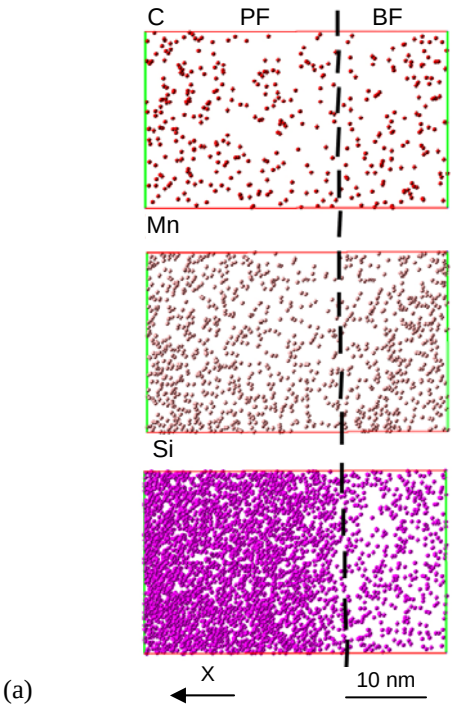

(a)

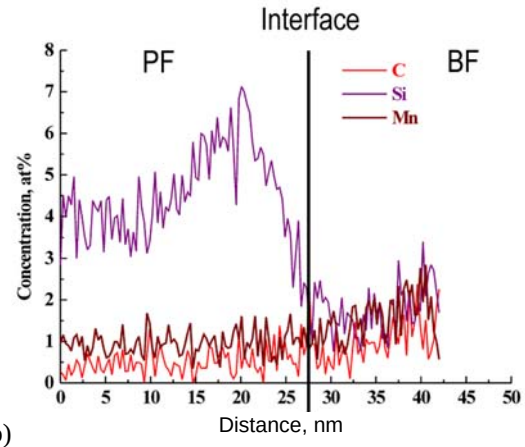

(b)

Figure 5: C, Mn and Si atom maps showing (a) polygonal ferrite/bainitic ferrite interface in the non-Nb TRIP steel and (b) corresponding X-direction concentration profile across the interface. PF is polygonal ferrite and BF is bainitic ferrite

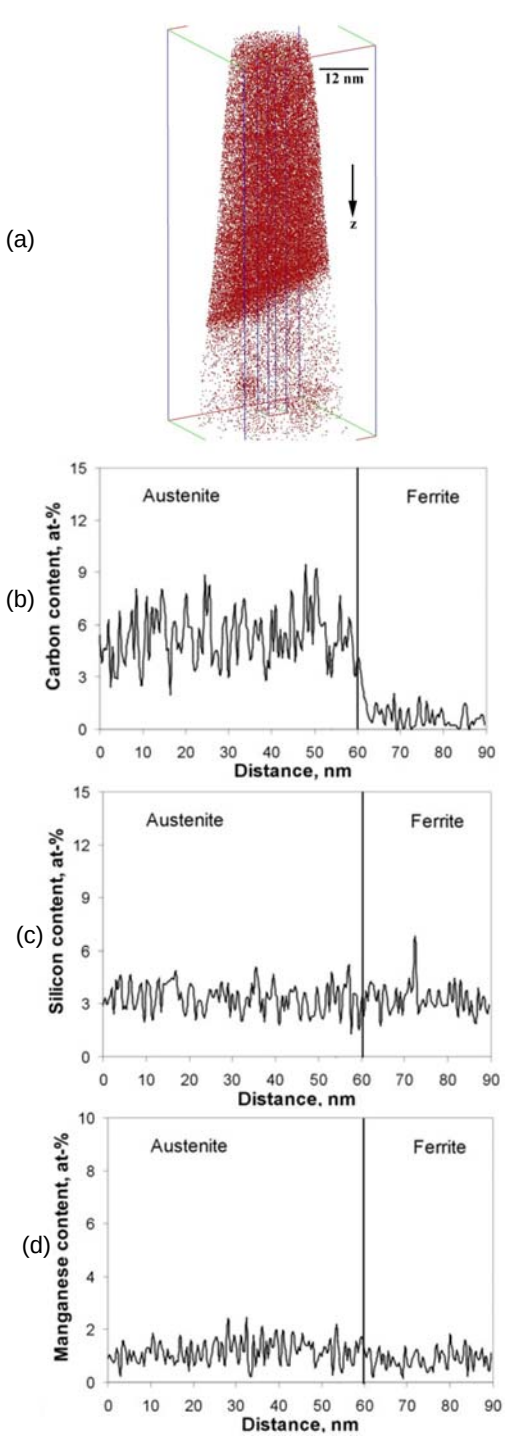

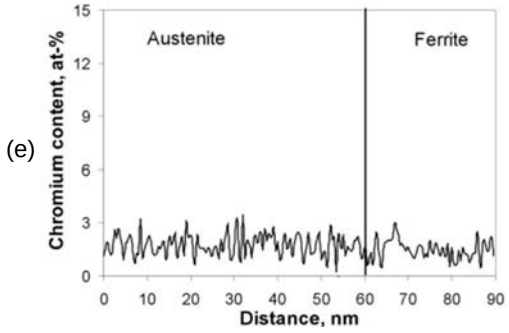

Figure 6: Carbon atom map (a) and corresponding concentration profiles ((b)-(e)) along the marked z-direction across the retained austenite/bainitic ferrite interface after isothermal bainite formation at 200°C. Adapted from Caballero *et al.* [7], Copyright 2007 with permission from Elsevier

APT was also used to elucidate the mechanism of carbon partitioning during a quench and partitioning treatment of intercritically annealed TRIP steels [17, 18]. The results support the enrichment of remaining austenite with carbon from freshly formed martensite, as the carbon level was significantly lower in martensite (~0.5 at.%) than in austenite (~3.6 at.%) [17].

Carbon Segregation at Defects

The displacive mechanism of bainite formation results in shape deformation accompanied by partial shape relaxation [19, 20]. This results in the formation of dislocations in and around the bainite, as well as twinning of adjacent regions of austenite [21, 22]. Excess carbon in bainitic ferrite, compared with the para-equilibrium values, is associated with trapping of carbon within defects (such as dislocations) in the matrix [23].

APT has provided direct evidence of carbon segregation to microtwins in retained austenite of bainitic steel (Figure 7) and of Cottrell atmospheres around dislocations in

bainitic ferrite (Figure 8), as shown by Caballero *et al.* [7]. In Figure 8(a), the top left carbon-enriched region is austenite, whereas the carbon-depleted bottom right region is bainitic ferrite.

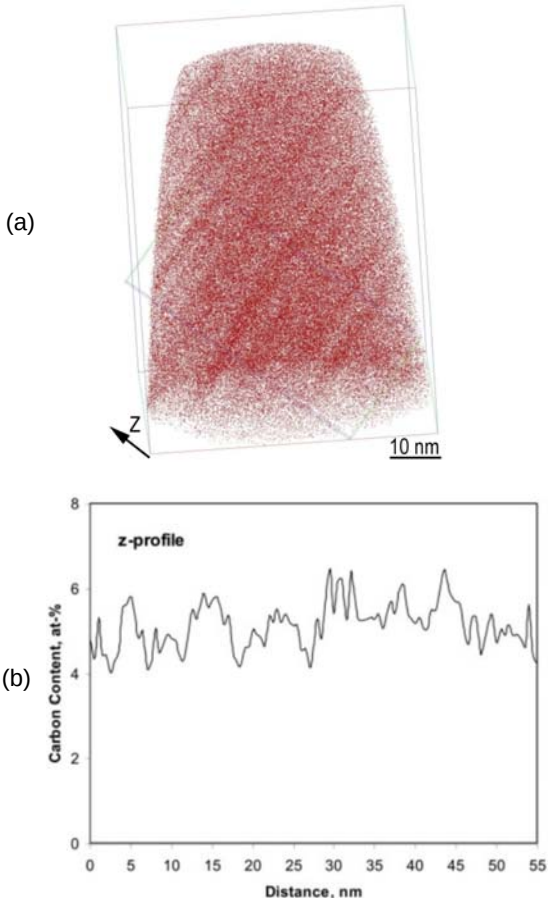

Figure 7: Carbon atom map (a) and z concentration profile (b) showing segregation of carbon at microtwins in retained austenite for a sample transformed at 300^{o}C for 4h. Reprinted from Caballero *et al.* [7], copyright (2007) with permission from Elsevier

The carbon-enriched linear features adjacent to the austenite/bainitic ferrite interface are deemed to be carbon segregation around dislocations (Figures 8(a) and 8(b)).

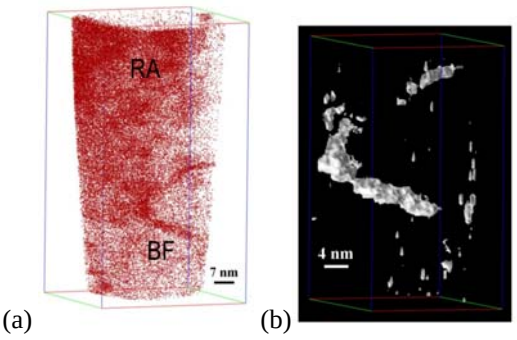

Figure 8: Carbon atom map (a) and 5% isoconcentration surface (b) of dislocations in the vicinity of a ferrite/austenite interface. RA is retained austenite; BF is bainitic ferrite. Reproduced from Caballero *et al.* [7], copyright 2007 with permission from Elsevier

Segregation of carbon to dislocations was observed in polygonal ferrite and bainite of non-alloyed CMnSi TRIP steel both after thermomechanical processing and after a subsequent bake hardening treatment [24, 25]. An example of such Cottrell atmospheres is given in Figure 9. No other solute segregation at dislocations was detected, either in TRIP or bainitic steels (Figure 9(b)).

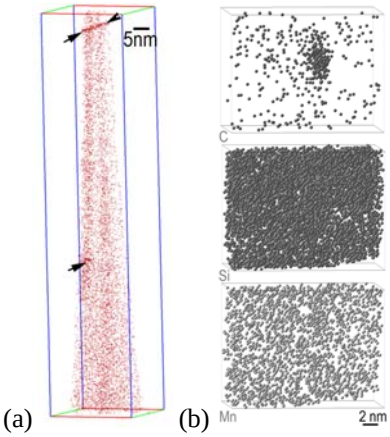

Figure 9: C atom map showing the presence of Cottrell atmospheres in polygonal ferrite of non-Nb TRIP steel after TMP (a) and projected C, Mn and Si selected atom maps showing segregation of C abound dislocation (b)

The carbon concentration in the cores of atmospheres observed in TRIP and bainitic steels ranged from 2 to 9 at.%, which is in agreement with predicted values by Cochardt et al. [26] of 6–7 at.% in the region of within one Burgers vector around the dislocation core.

Clustering and Fine Precipitation

Both clustering and precipitation are important microstructural events, the understanding of which is essential for both design of new steel compositions and processing routes. In TRIP steels alloyed with Nb, Mo and/or Al, C-Nb-Mo-Fe clusters and precipitation formation was studied in-depth by APT [27].

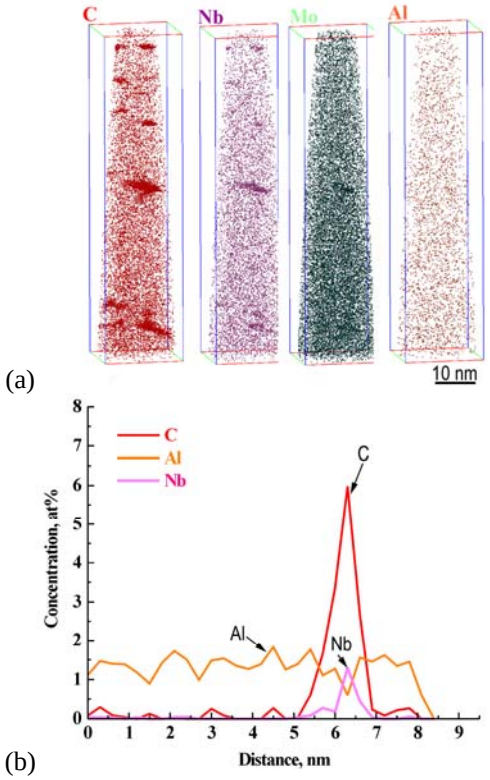

Figure 10: C, Nb, Mo and Al atom maps showing clusters and precipitates in NbMoAl TRIP steel after TMP (a) and representative concentration profile across a NbC particle (b)

APT provides not only three-dimensional information about size, morphology and density of these features, as can be seen in Figure 10, but allows the evolution of composition either as a function of size or processing schedule to be followed. In the NbAl steel after TMP, both clusters and fine particles in polygonal ferrite and bainitic ferrite were C-rich Nb-C. With an increase in size, the fine particles composition approached that of a stoichiometric NbC precipitate. In Nb- and Mo-containing TRIP steels, a similar trend of a decrease in C content with increase in precipitate size was observed (Figure 11(a)). However, the coarsest particles observed by APT were iron carbides with partial substitution of Fe by Nb and/or Mo.

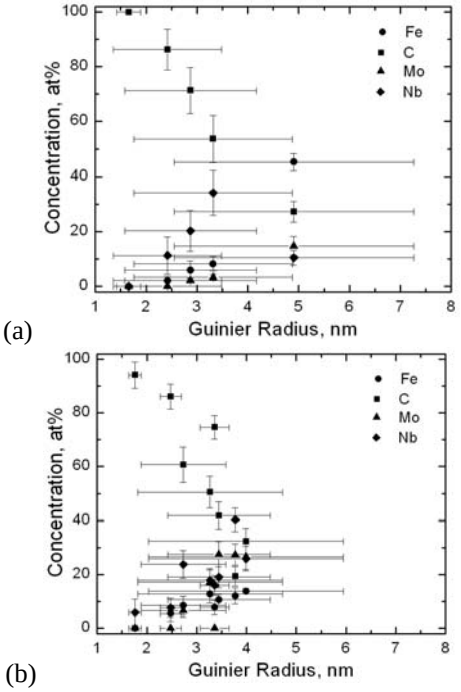

Figure 11: Summary of evolution of composition of clusters and fine precipitates with size observed in polygonal ferrite and bainitic ferrite of all TRIP steels after TMP (a) and pre-straining and bake hardening (b)

In retained austenite/martensite of all TRIP steels in TMP condition, fine C-clusters were observed (Figure 12(a)), the majority of which contain 80–100% C (Figure 13(a)). Slightly coarser particles (r_G = 2–3 nm) had a composition close to Fe_3C with traces of Nb and Mo. It could be suggested that they are the result of autotempering of the martensite formed from chemically unstable austenite either at the isothermal hold temperature or on cooling to room temperature.

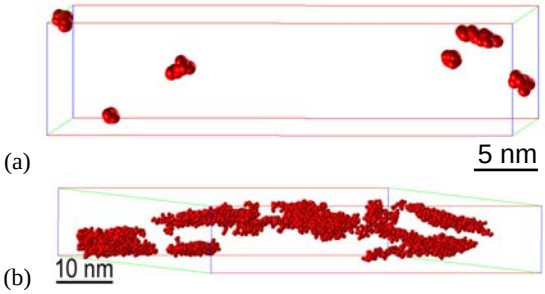

Figure 12: C-rich clusters (a) and carbides (b) in martensite of a TRIP steel after TMP (a) and pre-straining and bake hardening (b). All matrix atoms have been removed by a maximum separation method with d_{max} = 0.5 nm

Effect of Heat Treatment on the Microstructure

After pre-straining and bake hardening of the TRIP steels, no clusters containing 100% C were detected and the observed clusters and fine precipitates of comparable size to those present in the TMP condition contained less carbon and iron (Figure 11(b)). Fe-rich (Fe, Nb, Mo)C particles were no longer present in the microstructure, whereas particles were more enriched in Nb and Mo compared with the TMP condition, having compositions close to $MC_{0.8}$ and to stoichiometric MC, where M was Nb, Mo and Fe in various proportions. Despite a low heat treatment temperature, coarsening of clusters and precipitates was evident.

Decomposition of martensite continued during bake hardening with the formation of plate-like iron carbides (Figure 12(b)). The number density of clusters/fine carbides has increased by more than an order of magnitude compared with the TMP condition. A significant number of coarse carbides with composition close to stoichiometric Fe_3C and traces of Nb and Mo were present in the microstructure of the steels (Figure 13(b)). The results have shown a continuous evolution of cluster/precipitate composition with increase of Fe:C ratio during coarsening.

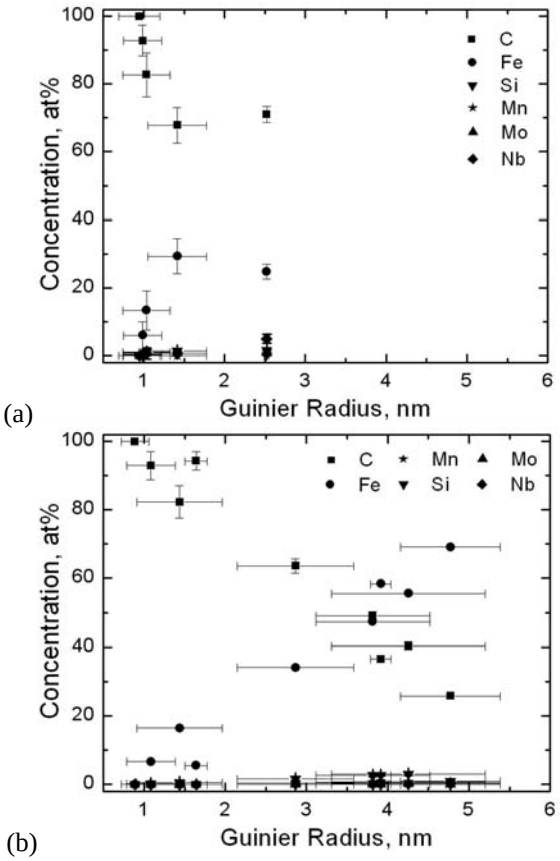

Figure 13: Summary of size effect on the composition of clusters/fine precipitates in martensite of TRIP steels after TMP (a) and after pre-straining and bake hardening (b)

APT allowed analysis of atomic redistribution of elements between austenite and bainitic ferrite during subsequent tempering of bainitic steel (Figure 14). As was reported by Caballero *et al.* [8, 15], no redistribution of any substitutional elements between austenite and BF was observed after tempering at 400°C for 1 h and only partitioning of chromium was detected after 30 min. at 450°C (Figure 14(b)). At the same time, austenite started to decompose; its carbon content is reduced and the presence of ε -carbide (~30 at.%C) was detected in ferrite (Figure 14). Contrary to the behaviour of substitutional elements, carbon readily partitions between the phases during tempering (Figure 14(b)). These results led to the conclusion that retained austenite decomposes into ferrite and cementite or fine pearlite before local equilibrium is reached at the interface [8, 15].

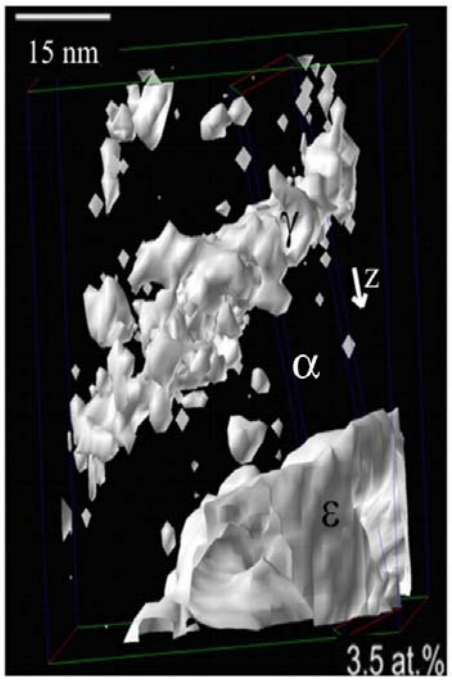

(a)

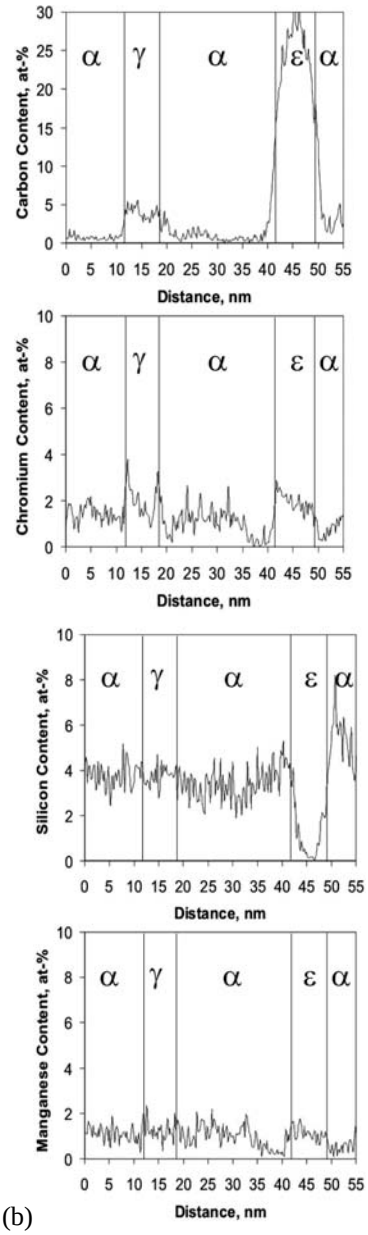

(b)

Figure 14: A 3.5 at.% carbon iso-concentration surface (a) and concentration profiles (b) along marked z-direction across austenite/bainitic ferrite interface after tempering at 450°C for 30 min. γ is retained austenite, α is bainitic ferrite and ε is ε-carbide. Reprinted from Caballero *et al.* [8], copyright 2008, with permission from Elsevier

CONCLUSION

It has been shown that APT is a powerful technique which allows a detailed characterisation of fine microstructural features in steels at the atomic level. It provides a complete chemical and 3D-spatial information on solute segregation, clustering and fine precipitation, which is impossible to obtain by any other technique.

ACKNOWLEDGEMENTS

The authors would like to thank Dr. F.G. Caballero, CENIM-CSIC for permission to use the results on bainitic steel. The authors acknowledge the technical support by Mrs. K.F. Russell, ORNL and Mr. T. Schambron, UOW. Atom probe research at the Oak Ridge National Laboratory SHaRE User Facility was sponsored by the Scientific User Facilities Division, Basic Energy Sciences, U.S. Department of Energy.

REFERENCES

[1] Kelly, T.F., Camus, P.P., Larson, D.J., Holzman, L.M. and Bajikar, S.S.: *U.S. Patent*, Serial No. 08/272204; (1995).

[2] Miller, M.K., Atom Probe Tomography, in *Handbook of Microscopy for Nano-technology*, Eds. Yao, Nan and Wang, Z.L., Kluwer Academic Press, New York, NY, (2005), p. 742.

[3] Miller, M.K., *Microsc. Res. Techn.*, Vol. 69, (2006), p. 359.

[4] Timokhina, I.B., Hodgson, P.D. and Pereloma, E.V., *Metall. Mater. Trans. A*, Vol. 35A, (2004), p. 2331.

[5] Timokhina, I.B., Hodgson, P.D. and Pereloma, E.V., *Metall. Mater. Trans. A*, Vol. 34A, (2003), p. 2331.

[6] Pereloma, E.V., Timokhina, I.B., Miller, M.K. and Hodgson, P.D., *Acta Mater.*, Vol. 55, (2007), p. 2587.

[7] Caballero, F.G., Miller, M.K., Babu, S.S. and Garcia-Mateo, C., *Acta Mater.*, Vol. 55, (2007), p. 381.

[8] Caballero, F.G., Miller, M.K., Garcia-Mateo, C., Capdevila, C. and Babu, S.S., *Acta Mater.*, Vol. 56, (2008), p. 188.

[9] Miller, M.K., *Atom Probe Tomography*, Kluwer, Academic/Plenum Press, New York, (2000).

[10] Peet, M., Babu, S.S., Miller, M.K. and Bhadeshia, H.K.D.H., *Scripta Mater.*, Vol. 50, (2004), p.1277.

[11] Caballero, F.G. and Bhadeshia, H.K.D.H., *Current Opinion in Solid State and Materials Science*, Vol. 8, (2004), p. 251.

[12] Oblak, J.M. and Hehemann, R.F., *Transformations and Hardenability in Steels*, Climax Moly. Ann Arbor, (1967), p.15.

[13] Bhadeshia, H.K.D.H. and Edmonds, D.V., *Acta Metall.*, Vol. 28, (1980), p. 1265.

[14] Bhadeshia, H.K.D.H., *Acta Metall.*, Vol. 29, (1981), p. 1117.

[15] Caballero, F.G., Miller, M.K. and Garcia-Mateo, C. 1, *Mater. J., Sci.*, 2008, DOI: 10.1007/s10853-007-2157-x.

[16] Stark, I., Smith, G.D.W. and Bhadeshia, H.K.D.H., *Metall. Trans. A.*, Vol. 21A, (1990), p. 837.

[17] Clarke, A.J., Speer, J.G., Hackenberg, R.E., Miller, M.K., Edmonds, D.V., Rizzo, F.C., Matlock, D.K. and Moor, E. De, *Acta Mater.*, Vol. 56, (2008), p. 16.

[18] Edmonds, D.V., He, K., Miller, M.K., Rizzo, F.C., Clarke, A., Matlock, D.K. and Speer, J.G., *Mater. Sci. Forum*, Vol. 539-543, (2007), p. 4819.

[19] Shrinivasan, G.R. and Wayman, C.M., *Acta Metall.*, Vol. 16, (1968), p. 621.

[20] Bhadeshia, H.K.D.H., *Bainite in Steels, 2nd. edition*, IOM Communications, The University Cambridge Press, (2001).

[21] Nemoto, M., *High Voltage Electron Microscopy*. New York, Academic Press, (1974), p. 230.

[22] Sandvik, B.P.J. and Nevalainen, H.P., *Met. Techn.*, Vol. 15, (1981), p. 213.

[23] Kalish, D. and Cohen, M., *Mater. Sci. Eng.*, Vol. 6, (1970), p. 156.

[24] Pereloma, E.V., Russell, K.F., Miller, M.K. and Timokhina, I.B., *Scripta Mater.*, (2008), DOI 10.1016/ j.scriptamat.2008.02.002.

[25] Pereloma, E.V., Timokhina, I.B. and Miller, M.K., "Effect of Nb and Mo additions on the microstructure and mechanical properties of thermomechanically processed and bake hardened CMnSi TRIP steel," in *Proc. Int. Conference on New Developments on Metallurgy and Applications of High Strength Steels*, 26–28 May, (2008), Buenos Aires, Argentina (in press).

[26] Cochardt, A.W., Schoek, G. and Wiedersich, H., *Acta Metal.*, Vol. 3, (1955), p. 533.

[27] Pereloma, E.V., Timokhina, I.B., Russell, K.F. and Miller, M.K., *Scripta Mater.*, Vol. 54, (2006), p. 471.